International Journal of Mass Spectrometry 291 (2010) 152–158

Contents lists available at ScienceDirect

International Journal of Mass Spectrometry

journal homepage: www.elsevier.com/locate/ijms

SSITKA investigation of CO and H_2 competitive adsorption at PEM fuel cell anode catalysts

J.C. Davies[a,1], G. Tsotridis[a], M. Varlam[b], S. Valkiers[b,*], M. Berglund[b], P. Taylor[b]

[a] Institute for Energy, Joint Research Centre, European Commission, Postbus 2, 1755 ZG Petten (NL), The Netherlands
[b] Institute for Reference Materials and Measurements, Joint Research Centre, European Commission Retieseweg 111, B-2440, Geel (B), Belgium

ARTICLE INFO

Article history:
Received 30 December 2009
Received in revised form 1 February 2010
Accepted 2 February 2010
Available online 6 February 2010

Keywords:
SSITKA
CO adsorption/desorption
PEMFC anode catalyst
Pt
Ru

ABSTRACT

Steady-state isotopic transient kinetic analysis (SSITKA) experiments have been performed using the isotopic exchange between ^{13}CO and ^{12}CO to investigate the competitive adsorption of hydrogen and CO on commercial Pt and PtRu catalysts. PtRu alloys are known to be more tolerant fuel cell anode catalysts than platinum, in the instance where the hydrogen fuel contains ppm levels of CO. It has been recently demonstrated that there is a dynamic equilibrium between CO adsorbed on platinum or platinum/ruthenium nano-particles and CO in the gas phase. In this paper, the effect of the competitive adsorption between hydrogen and CO on this equilibrium has been demonstrated.

For 1400 ppm CO in hydrogen little difference was observed in the measured exchange rates for Pt and PtRu at room temperature, 9.91×10^{-4} for Pt compared to 1.15×10^{-3} for PtRu, however there is a significant effect observed at 100 ppm CO in hydrogen, where the rates on PtRu are considerably smaller than on Pt (3.61×10^{-4} desorption rate constant for PtRu and 5.49×10^{-4} for Pt).

The presented methodology using the SSITKA technique has demonstrated a novel way to measure these rate constants, and the implications of these measurements on the mechanistic understanding of the anode reaction are presented.

1. Introduction

At the anode of the proton exchange membrane fuel cell (PEMFC) hydrogen dissociation and subsequent oxidation to protons occurs. This electrode is generally platinum-based due to the high hydrogen oxidation currents obtained and the stability of platinum under the operating conditions of the fuel cells [1].

If the hydrogen used within the fuel cell is obtained from clean sustainable resources (such as that produced by electrolysis using electrical energy obtained from wind or solar power) then the only product of the fuel cell is water. However, if the hydrogen feed to the anode of the PEMFC is produced from reformation of hydrocarbons by partial oxidation or steam reforming this will produce hydrogen containing significant levels of both carbon monoxide and carbon dioxide. A variety of further stages of purification can be performed to remove the CO, but it is known that as little as ppm levels of CO in the anode feed gas can poison the hydrogen oxidation reaction on platinum by binding strongly to the platinum surface and blocking sites for hydrogen dissociation [2].

It has been demonstrated that alloying platinum with a second metal, usually ruthenium, can increase the tolerance of the anode to CO adsorption [3]. There are currently three main proposed mechanisms for this promotion:

(i) *The bifunctional effect* [4]: Alloying platinum with ruthenium, at an optimal ratio of 50:50 reduces the overpotential required for the oxidation of adsorbed CO to CO_2 [5–9]. This reduction in overpotential is associated with the dissociation of water being more facile on ruthenium than on platinum.
(ii) *The ligand effect*: Alloying platinum with ruthenium alters the chemical properties of the surface platinum due to electronic effects. It has been suggested that this weakening of the CO bond could affect the CO oxidation rate in mechanism (i) however, it has previously been demonstrated that the oxygen dissociation is the predominant effect with regard to that mechanism [10,11].
(iii) *The detoxification mechanism* [12–14]: It has been suggested that the electronic effect of alloying platinum with ruthenium, mentioned in mechanism (ii), can weaken the CO bond strength to a significant enough degree that the subsequent drop in the equilibrium coverage (via adsorption/desorption

* Corresponding author. Tel.: +32 014 571 639; fax: +32 014 571 863.
E-mail address: staf.valkiers@ec.europa.eu (S. Valkiers).
[1] Current address: Ilika Technologies Ltd., Kenneth Dibben House, Enterprise Road, University of Southampton Science Park, Chilworth, Southampton SO16 7NS, United Kingdom.

1387-3806/$ – see front matter © 2010 Elsevier B.V. All rights reserved.
doi:10.1016/j.ijms.2010.02.003

of CO from the gas phase) can lead to a "detoxification" effect on the catalyst particle surface.

It has recently been shown that there is a dynamic equilibrium between CO adsorbed on platinum or platinum/ruthenium catalysts, and CO in the gas phase, on a time-scale relevant to the behavior of fuel cell anodes [15,16].

Steady-state isotopic transient kinetic analysis (SSITKA) was developed initially by Happel [17], Bennett[18] and Biloen [19] as a technique for studying surface reactions and was proven to be a powerful tool for the determination of kinetics and of catalyst surface reaction intermediates *in situ*. The idea behind this technique is that steady-state conditions are maintained under isotopic transient operations and therefore the advantages of steady-state and of transient investigations are applied: steady-state methods measure overall performance and give an integrated picture of a reaction system but transient methods provide information on individual steps and have increased resolution. SSITKA is further based upon the detection of isotopic labels in the reactor effluent species versus time following a switch (step change) in the isotopic labeling of one of the reactant species in the reactor feed. In addition to maintaining isothermal and isobaric reaction conditions, the reactant and product concentrations and flow rates have to remain undisturbed during the step change. Thus, in the absence of isotopic mass effects, steady-state reaction conditions are maintained under isotopic transient operation. In this case, the use of isotopic tracing only requires that reactions do not change significantly during the isotopic transient period.

Steady-state isotopic transient kinetic analysis (SSITKA) experiments have been performed in this paper using the isotopic exchange between ^{13}CO and ^{12}CO to investigate the competitive adsorption of hydrogen and CO at concentrations relevant to PEM fuel cells. These experiments have been performed with the aim of more fully understanding the mechanisms involved in CO tolerance by providing rate constants relevant to the fuel cell anode reaction.

2. Theory

The reactions occurring at the fuel cell anode can be described as follows:

$$H_2 + 2* \leftrightarrow 2H_{ad} \quad (1)$$

$$CO + * \leftrightarrow CO_{ad} \quad (2)$$

$$H_2O + * \leftrightarrow H_2O_{ad} \quad (3)$$

$$H_2O_{ad} \rightarrow OH_{ad} + H^+ + e^- \quad (4)$$

$$OH_{ad} + CO_{ad} \rightarrow 2* + CO_2 + H^+ + e^- \quad (5)$$

$$H_{ad} \rightarrow * + H^+ + e^- \quad (6)$$

where * is the adsorption site on the catalyst surface.

In the simplified environment, without humidification or an induced potential, only the first two reactions can occur, the adsorption/desorption of CO and hydrogen for which the equilibrium rate constants, K_{CO} and K_{H_2}, can be defined.

For CO diluted with an inert gas, the Langmuir adsorption isotherm for associative adsorption can be defined as:

$$\theta_{CO} = \frac{K_{CO}p_{CO}}{1 + K_{CO}p_{CO}} \quad (7)$$

where θ is the coverage and p is the partial pressure.

However, when performing SSITKA experiments, both isotopically labeled and unlabeled CO are present in the system.

Therefore:

$$^{12}CO + * \leftrightarrow {}^{12}CO_{ad} \quad (8)$$

$$^{13}CO + * \leftrightarrow {}^{13}CO_{ad} \quad (9)$$

The following three expressions have previously been derived for isotopic exchange experiments involving CO adsorption/desorption in an inert diluent (i.e., where the diluent does not compete for adsorption sites with CO) [15]:

$$\frac{d\theta_{^{12}CO}}{dt} = k^+ p_{^{12}CO}\theta_* - k^- \theta_{^{12}CO} \quad (10)$$

$$\frac{d\theta_{^{13}CO}}{dt} = k^+ p_{^{13}CO}\theta_* - k^- \theta_{^{13}CO} \quad (11)$$

$$\theta_* = 1 - \theta_{^{13}CO} - \theta_{^{12}CO} \quad (12)$$

where k^+ is the rate constant for the adsorption process and k^- is the rate constant for the desorption process.

It should now be considered what will happen in the presence of hydrogen. There are three possible scenarios to consider for interpretation of the data which will be discussed below.

2.1. CO adsorption/desorption strongly predominates (effect of hydrogen diluent insignificant); no CO readsorption

After the isotopic switch occurs, in a situation where there is no significant readsorption of the desorbing gas, Eq. (10) reduces to:

$$\frac{d\theta_{^{12}CO}}{dt} = -k^- \theta_{^{12}CO} \quad (13)$$

and therefore,

$$\theta_{^{12}CO} = \theta^0_{^{12}CO} e^{-k^- t} \quad (14)$$

Note that at $t = 0$ the coverage of ^{12}CO is equivalent to the total CO coverage at this temperature and pressure, θ_{CO}, hence the standardized function for the decrease of the ^{12}CO isotope in the gas phase is:

$$C(t) = e^{-k^- t} \quad (15)$$

By analogous reasoning, the increase in the concentration of the ^{13}CO isotope can be given by:

$$C'(t) = 1 - e^{-k^- t} \quad (16)$$

These standardized functions are the transient curves of the two products for the simplest case of the adsorption–desorption process. The sum of these two normalized functions is at any moment equal to unity. These assumptions have been previously shown to be valid at low concentrations of CO in an inert diluent at room temperature (where insignificant readsorption rates were observed) [15]. Under these conditions, no dependence on flow rate was observed above 20 mL/min.

2.2. CO adsorption/desorption strongly predominates (effect of hydrogen diluent insignificant); CO readsorption

In this scenario the adsorption term for the desorbing species must be considered and Eq. (10) must be considered in its entirety.

This scenario can be distinguished from Section 2.1 by a strong dependence on flow rate. It has been previously proposed [20,21], that the concentration of ^{12}CO in the gas phase will decrease as:

$$C(t) = \frac{\theta_{CO}k^-}{q + (\theta_{CO}k^-)/C_0} \exp\left[-\frac{k^-}{1 + (\theta_{CO}k^-)/qC_0}t\right] \quad (17)$$

where q represents the flow rate and C_0 denotes the concentration of ^{12}CO at $t = 0$ (i.e., at the point of isotopic switch). Therefore the initial gradient of a semi-logarithmic plot can now be defined as an apparent desorption rate constant k^{app} where:

$$k^{app} = \frac{k^-}{1 + (\theta_{CO}k^-)/qC_0} \quad (18)$$

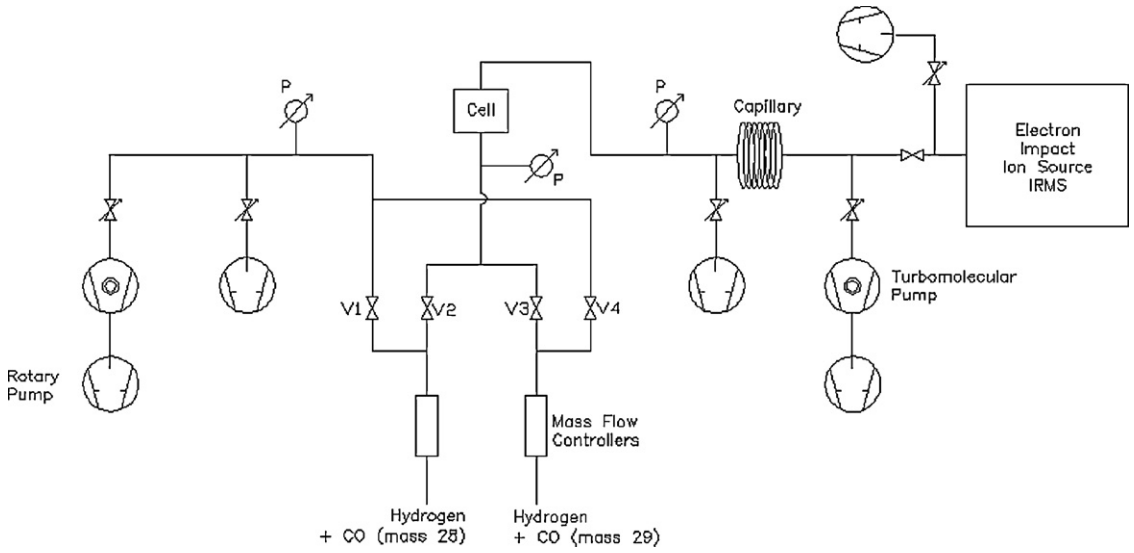

Fig. 1. Schematic of the gas inlet system used in the experiments.

Rearranging gives:

$$\frac{1}{k^{app}} = \frac{1}{k^{-}} + \frac{\theta_{CO}}{C_0}\frac{1}{q} \tag{19}$$

meaning that a plot of $1/k^{app}$ versus $1/q$ should provide a linear response, with an intercept of $1/k^{-}$, the unidirectional desorption rate constant.

The above model has previously been used when there was significant readsorption (at temperatures of 50 °C and higher) at concentrations of 1000 ppm CO in argon [21]. It has also been demonstrated that no significant difference in the rate of exchange of CO at any given pressure is observed on going from Pt to PtRu catalysts when the diluted gases used is argon since the CO states [16].

2.3. Competition with H_2

When hydrogen is used as the diluent gas, as has been performed in this study, we would expect to see a deviation from the behavior proposed by the two models given above. Experiments performed at a single flow rate at room temperature presented in [16] by a pseudo-SSITKA approach have indeed observed a disparity between the data observed with Ar and H_2 as carrier gas.

In the instance where competitive adsorption occurs, the isotherms governing CO and hydrogen coverage are, by analogy to Eq. (7):

$$\theta_{CO} = \frac{K_{CO}p_{CO}}{1 + K_{CO}p_{CO} + \sqrt{K_{H_2}p_{H_2}}} \tag{20}$$

$$\theta_{H} = \frac{\sqrt{K_{H_2}p_{H_2}}}{1 + K_{CO}p_{CO} + \sqrt{K_{H_2}p_{H_2}}} \tag{21}$$

In real terms for these experiments, this will lead to a deviation from the expected behavior according to scenario 2.2.

3. Experimental methods

A gas inlet system has been set-up for the SSITKA analysis system as shown in Fig. 1. Gas mixtures were prepared from the highest available purity CO, hydrogen and ^{13}C isotopically enriched CO. Flow rates used for the experiments ranged from 10 mL/min to 100 mL/min.

The samples used were commercial Pt/C and PtRu/C from Electrochem Inc. with metal loadings of 1 mg/cm^2. These consist of the nanoparticulate metal supported on Vulcan carbon powder and subsequently bound to a Toray carbon sheet gas diffusion layer using a Teflon binder (this is more resistant to temperature than the Nafion binder which is necessary in the full membrane electrode assembly (MEA)).

Initially, using the set-up presented in Fig. 1, a flow of a neutral gas (N_2) was used in order to determine the response time of the system for subtraction from the obtained data. Assuming that no chemical or physical process is occurring, the transient curve of the monitored mass-to-charge 28 u/e signal (where u is the atomic mass unit and e is the electron charge) provides an accurate background subtraction of the experimental system. All the experimental spectra which have been acquired for CO–hydrogen gaseous mixtures were mathematically treated by subtracting the nitrogen transient curve occurred under the relevant conditions.

Experiments were then performed according to the following methodology. A flow of unlabelled CO in hydrogen was passed through the cell (valve V2 open, valve V1 closed, Pcell = 1 bar). A mixture of isotopically enriched CO in hydrogen, with the same total CO concentration, was flowed through a "dummy" line simultaneously (valve V4 open, valve V3 closed) under the same conditions of pressure and flow. After a time (usually in excess of 1 h, in order to obtain an initial state of the surface covered with ^{12}CO), the valves were switched so that the isotopically labeled mixture flowed through the cell, and the unlabelled mixture to the dummy line (valves V1 and V3 open, valves V2 and V4 closed). The m/e = 28 u/e and 29 u/e response was then measured using the electron impact ion source IRMS. The experimental set-up has been designed and built to allow the flow rate adjusting at the required level and also to prevent any flow rate and pressure variation during the switching between the two flow channels. Along the home-designed inlet system, the pressure of the gaseous mixture decreased in a controlled way from ~16 bars in the gas ampoules to 10^{-8} mbar in the mass spectrometric electron impact ion source, but keeping the flow rate constant. The mass-to-charge 28 u/e and 29 u/e signals have been acquired over a 2-h period. The output of every experiment was a matrix data with the time-intensities values which were used afterwards as the basis for the mathematical treatment.

This procedure was followed for different flow rates (10–100 sccm), concentrations for both Pt/C and $Pt_{0.5}Ru_{0.5}/C$ as described in the following section.

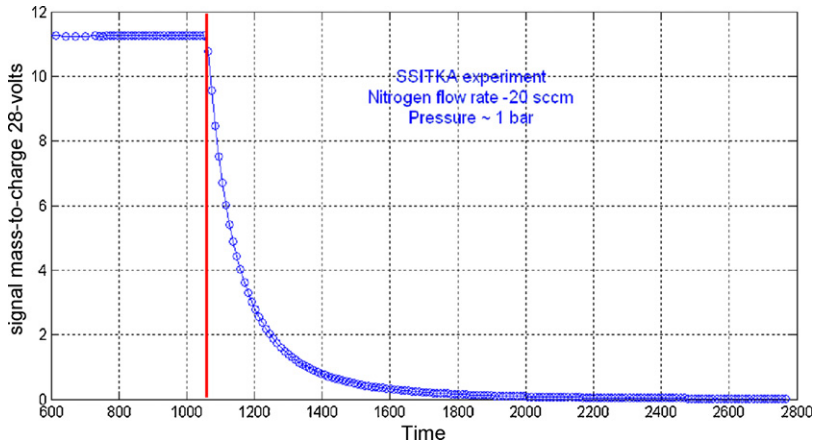

Fig. 2. Nitrogen signal in function of time (the red line is indicating the 'start time'). (For interpretation of the references to color in this figure legend, the reader is referred to the web version of the article.)

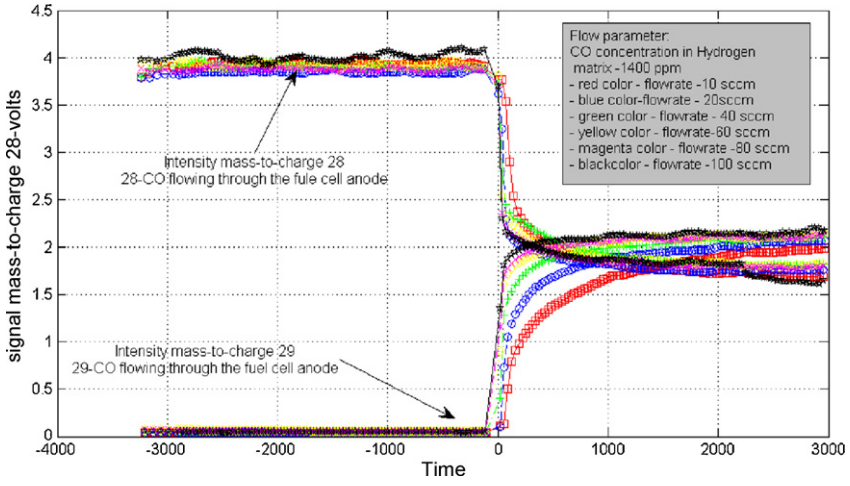

Fig. 3. Flow dependent CO exchange on Pt catalysts at 25 °C and 1400 ppm CO in H_2.

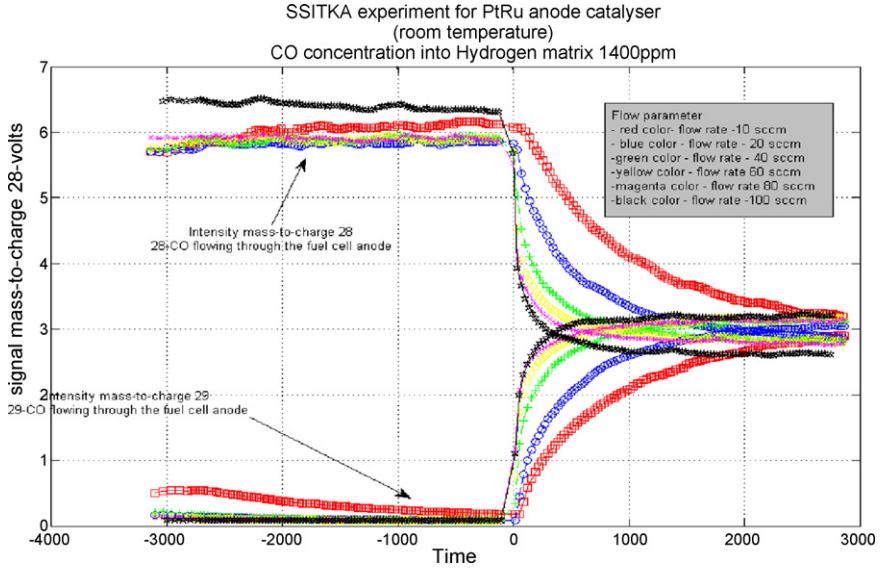

Fig. 4. Flow dependent CO exchange on PtRu catalysts at 25 °C and 1400 ppm CO in H_2.

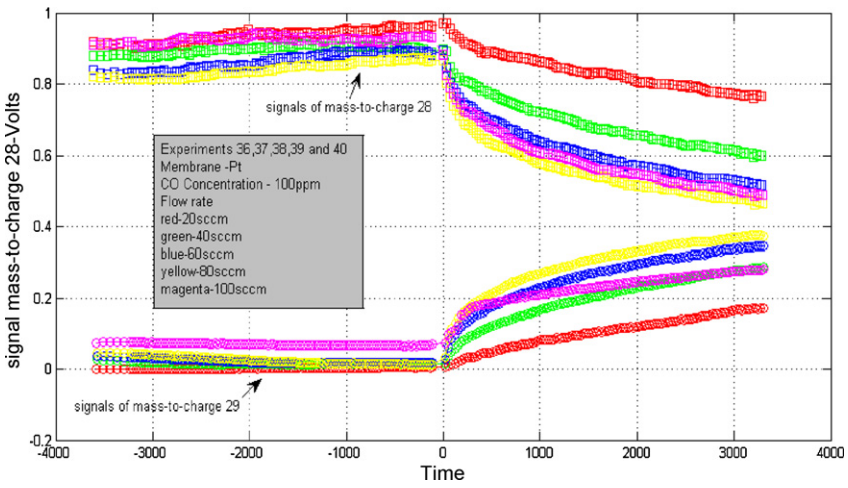

Fig. 5. Flow dependent CO exchange on Pt catalysts at 25 °C and 100 ppm CO in H_2.

4. Results

As outlined above, experiments have been performed for two types of commercial catalysts—Pt and PtRu, and for two different concentrations of CO in hydrogen—1400 ppm and 100 ppm.

As previously described in Section 3, the response time of the experimental set-up was determined using nitrogen as an inert gas (it is known to be an inert diluent at the fuel cell anode). An example of the nitrogen signal (mass-to-charge (m/e) ratio of 28 u/e), for an initial flow of 20 mL/min, is shown in Fig. 2. The calculated area below the nitrogen signal time dependence has been subtracted from the CO/H_2 measurements for all subsequent data analysis.

Initially the CO exchange experiment was performed with the Pt samples for a concentration of 1400 ppm CO in hydrogen at 25 °C as shown in Fig. 3. Data was obtained for a range of flow rates and the flow rate dependence was observed. This experiment was repeated for the PtRu catalyst (as shown in Fig. 4).

Data was then obtained for 100 ppm CO in hydrogen at 25 °C for both the Pt (Fig. 5) and the PtRu (Fig. 6) catalysts. This is the typical order of magnitude of CO concentration at which low temperature PEM fuel cells are able to operate with the use of more CO-tolerant PtRu catalysts. However, at these concentrations, the pure Pt catalysts are known to poison very quickly.

To determine the kinetic parameters the change in the mass/charge signal of 29 u/e was used. This is more accurate than using the mass/charge signal of 28 u/e, as the mass/charge signal of 29 u/e starts from the background zero value. If there is a slight difference in the two concentrations of the initial gases then this error will be incorporated into the mass/charge signal of 28 u/e.

The experiment switch which has been performed with an inert gas (nitrogen) to determine the lag time for the experiment when there is no adsorption–desorption event has been treated by analogy to Eq. (16) and therefore, the regression function for this normalized nitrogen result is:

$$y_{\text{nitro}} = 1 - a_{\text{nitro}}.e^{-(t/b_{\text{nitro}})} \tag{22}$$

These values were determined for each flow rate used and subtracted from the mass 29 experimental data prior to the fitting of that data. They are given in Table 1.

The exponential regression which was then applied to the mass 29 experimental data for the two different concentrations and catalyst materials was therefore:

$$y_{29} = 1 - a_{29}.e^{-(t/b_{29})} \tag{23}$$

where a_{29} and b_{29} are the values listed in Table 1.

By comparison of the exponential term in Eq. (23) with Eqs. (17)–(19) it can be seen that $1/b = k_{\text{app}}$, therefore a plot of b versus $1/q$ should provide an intercept of $1/k^-$ and therefore a value for the unidirectional rate constant for the desorption rate for these

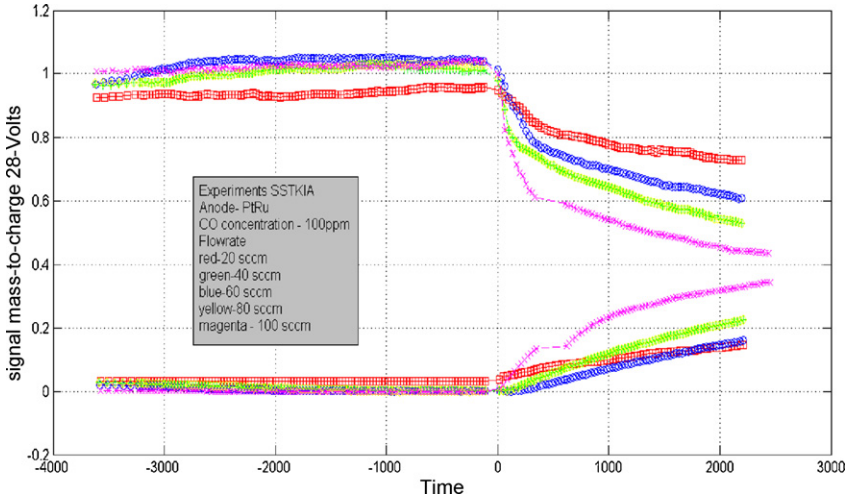

Fig. 6. Flow dependent CO exchange on PtRu catalysts at 25 °C and 100 ppm CO in H_2.

Table 1
Coefficients for the data obtained at room temperature.

Flow rate (sccm)	CO concentration (ppm)	Catalyst	Nitrogen		Hydrogen + CO	
			a_{nitro}	b_{nitro}	a_{29}	b_{29}
10	1400	Pt	9.9144	359.0264	0.2845	1358.02
20	1400	Pt	23.4874	251.5877	0.2267	1177.85
40	1400	Pt	56.8516	189.3382	0.1963	1104.52
60	1400	Pt	85.3862	166.8216	0.1744	1065.81
80	1400	Pt	95.2661	157.0364	0.1582	1020.37
100	1400	Pt	95.6176	152.213	0.1644	1069.65
10	1400	PtRu	9.9144	359.0264	0.3357	1520.39
20	1400	PtRu	23.4874	251.5877	0.2537	1150.02
40	1400	PtRu	56.8516	189.3382	0.192	1024.12
60	1400	PtRu	85.3862	166.8216	0.1717	982.82
80	1400	PtRu	95.2661	157.0364	0.1595	972.54
100	1400	PtRu	95.6176	152.213	1.1567	934.80
20	100	Pt	23.4874	251.5877	0.534	3036.02
40	100	Pt	56.8516	189.3382	0.4429	2511.03
60	100	Pt	85.3862	166.8216	0.3969	2238.94
80	100	Pt	95.2661	157.0364	0.3743	2127.3
100	100	Pt	95.6176	152.213	0.3104	2026.1
20	100	PtRu	23.4874	251.5877	0.3518	4776.7
40	100	PtRu	56.8516	189.3382	0.5933	3879.03
60	100	PtRu	85.3862	166.8216	0.5331	3314.92
80	100	PtRu	95.2661	157.0364	0.5329	3334.43
100	100	PtRu	95.6176	152.213	0.5252	3167.04

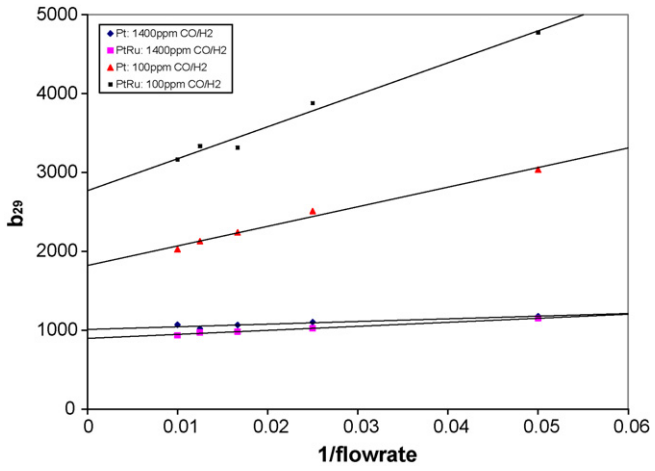

Fig. 7. Plot of b_{29} versus $1/q$ for Pt and PtRu catalysts under different concentrations of CO in hydrogen.

conditions can be obtained. The plot of b_{29} versus $1/q$ is given in Fig. 7.

From this chart the y-intercepts for the individual sets of conditions can be determined, and the unidirectional rate constants can be derived as given in Table 2.

It can be observed that at 1400 ppm there is little difference between the observed rates on Pt and PtRu, however at the lower concentration of 100 ppm it is clear that the rate of exchange of CO is considerably smaller on PtRu than on Pt. Similar behavior was also observed in [16] for 100 ppm and 1000 ppm CO in hydrogen using a pre-dosing technique (rather than traditional SSITKA) however, in this previous paper data was only obtained for a single flow rate (20 mL/min) under the assumption that the exchange rate was independent of flow rate at these concentrations. Whilst it can be seen from our data that this will give a relatively accurate value at 1000 ppm (the gradient of the plot is very "flat"), it is clearly not the case in our experiments at 100 ppm where the rate becomes more strongly dependent on mass transfer.

Table 2
Derived rates for the four sets of data.

Catalyst	Concentration (CO in H_2) (ppm)	Intercept	k^- (s^{-1})
Pt	1400	1009	9.91×10^{-4}
PtRu	1400	872	1.15×10^{-3}
Pt	100	1821	5.49×10^{-4}
PtRu	100	2769	3.61×10^{-4}

5. Discussion

In this study we have demonstrated that fast-switching SSITKA measurements can be performed to provide information on the adsorption/desorption rates of CO from Pt and PtRu catalysts at relevant concentrations of CO in hydrogen, therefore providing information regarding the competitive adsorption of these two species on Pt and PtRu. It is proposed that the adsorption/desorption rate of CO is important in controlling the equilibrium coverage of CO under the operating conditions of the fuel cell and therefore the subsequent rate of hydrogen oxidation.

Experiments have been performed at two concentrations; 1400 ppm and 100 ppm CO in hydrogen on both platinum and platinum/ruthenium catalysts. From fitting to the experimental data of the exponential increase in the desorbing CO ($m/e = 29\ u/e$ signal) it can be seen that there is very little difference in the rate of exchange on Pt and PtRu at the higher CO concentration. In [16] it was also observed that at higher concentrations of CO there is little difference in behavior between CO in hydrogen and in an inert diluent, implying that CO adsorption predominates. This would imply that scenario 2.2, outlined in Section 2, is a good approximation at a concentration of 1400 ppm in hydrogen.

However, when the concentration is lowered to 100 ppm, there is increased competition between the hydrogen and CO and the subsequent rate of exchange on the PtRu surface is significantly lowered compared to the rate on pure Pt.

It is most likely that this originates from lower equilibrium coverage for CO on the PtRu catalyst, which will naturally be beneficial for the hydrogen oxidation reaction under these conditions. It has previously been shown that the partial pressure of CO, the equilibrium coverage and the desorption rate are all strongly linked

parameters for these systems [15]. It is clear that towards lower concentrations of CO in hydrogen, the increased competition for sites is leading to a lower exchange rate for CO. At concentrations from 100 ppm CO upwards it has been shown that the rates of exchange under dry conditions are larger than the measured rates of oxidation of CO performed in electrochemical half-cells [15]. It is the balance between these two kinetic processes as lower concentrations of CO are reached, that will be the important factor in determining the relevant mechanism for CO tolerance.

Furthermore, it would also be interesting to look at the effect of temperature, humidification of the gas stream (the inclusion of a third adsorption species), and eventually to aim to perform such exchange experiments in a single cell arrangement.

Finally, if novel catalyst materials could be made available, the comparison of the fundamental kinetic parameters of such novel materials with those obtained from the industrial standard catalysts could provide additional information regarding the potential of the novel materials as CO-tolerant PEM fuel cell catalysts.

6. Conclusions

Steady-state isotopic transient kinetic analysis experiments were performed for the CO exchange process in hydrogen carrier gas at 1400 ppm and 100 ppm concentrations at a range of flow rates.

A dependence on flow rate was observed under all conditions. Rate constants for the desorption process were obtained by extrapolation of the data assuming a Langmuirian model.

For 1400 ppm CO in hydrogen little difference was observed in the measured exchange rates for Pt and PtRu at room temperature, however there is a more significant effect observed at 100 ppm CO in hydrogen, where the rates on PtRu are considerably slower than on Pt. This can be attributed to increased competition on PtRu for CO and H adsorption, leading to a lower equilibrium coverage of CO on the PtRu surface.

Acknowledgements

The authors would like to thank Roberto Bove, Aurelien Pitois and Marc Steen for a critical reading of the manuscript. This document does not represent the view of the European Commission. Any interpretations or opinions contained in this document are solely those of the authors.

References

[1] W. Vogel, J. Lundquist, P. Ross, P. Stonehart, Electrochim. Acta 20 (1975) 79.
[2] H. Igarashi, T. Fujino, M. Watanabe, J. Electroanal. Chem. 391 (1995) 119.
[3] H.F. Oetjen, V.M. Schmidt, U. Stimming, F. Trila, J. Electrochem. Soc. 143 (1996) 3838.
[4] M. Watanabe, S. Motoo, J. Electroanal. Chem. 60 (1975) 267.
[5] H.A. Gasteiger, N. Markovic, P.N. Ross, E.J. Cairns, J. Phys. Chem. 98 (1994).
[6] H.A. Gasteiger, P.N. Ross, E.J. Cairns, Surf. Sci. 293 (1993) 67.
[7] H.A. Gasteiger, N. Markovic, P.N. Ross, E.J. Cairns, Electrochim. Acta 39 (1994) 1825.
[8] H.A. Gasteiger, N. Markovic, P.N. Ross, J. Phys. Chem. 99 (1995) 8290.
[9] H.A. Gasteiger, N. Markovic, P.N. Ross, J. Phys. Chem. 99 (1995) 16757.
[10] C. Lu, C. Rice, R.I. Masel, P.K. Babu, P. Waszczuk, H.S. Kim, E. Oldfield, A. Wieckowski, J. Phys. Chem. B 106 (2002) 9581.
[11] J.C. Davies, B.E. Hayden, D.J. Pegg, Surf. Sci. 467 (2000) 118.
[12] H. Igarashi, T. Fujino, Y.M. Zhu, H. Uchida, M. Watanabe, Phys. Chem. Chem. 3 (2001) 306.
[13] M. Watanabe, Y.M. Zhu, H. Igarashi, H. Uchida, Electrochemistry 68 (2000) 244.
[14] P. Wolohan, P.C.H. Mitchell, D. Thompsett, S.J. Cooper, J. Mol. Catal. A 119 (1997) 223.
[15] J.C. Davies, R.M. Nielsen, L.B. Thomsen, I. Chorkendorff, A. Logadottir, Z. Lodziana, J.K. Norskov, W.X. Li, B. Hammer, S.R. Longwitz, J. Schnadt, E.K. Vestergaard, R.T. Vang, F. Besenbacher, Fuel Cells 4 (2004) 309.
[16] J.C. Davies, J. Bonde, A. Logadottir, J.K. Norskov, I. Chorkendorff, Fuel Cells 5 (2005) 429.
[17] J. Happel, J. Chem. Eng. Sci. 33 (1978) 1567.
[18] C.O. Bennett, in: A.T. Bell, L.L. Hegedus (Eds.), ACS Symposium Series, vol. 178, American Chemical Society, Washington, DC, 1982, p. 1.
[19] P. Biloen, J. Mol. Catal. 21 (1983) 17.
[20] M. Xu, E. Iglesia, J. Phys. Chem. B 102 (1998) 961.
[21] J.C. Davies, G. Tsotridis, J. Phys. Chem. C 112 (2008) 3392.